

Magnetization reversal and spin reorientation in Fe/Cu(100) ultrathin films

E. Mentz, A. Bauer, T. Günther, and G. Kaindl

Institut für Experimentalphysik, Freie Universität Berlin, Arnimallee 14, D-14195 Berlin, Germany

(Received 19 September 1997; revised manuscript received 30 September 1998)

The magnetization reversal in perpendicular applied magnetic fields in low-temperature grown Fe/Cu(100) ultrathin films was studied *in situ* by magneto-optical Kerr effect, Kerr-microscopy, and scanning tunneling microscopy. It was found that the onset of long-range ferromagnetic order at ≈ 0.9 monolayers (ML) is related to the coalescence of bilayer islands of Fe. Below 3.8 ML, the magnetization-reversal process takes place in a narrow field range and is characterized by domain-wall motion. While the domain boundaries are rather smooth at thin films, domains get increasingly irregularly shaped above 3 ML, which is assigned to a decrease of the domain-wall energy. At the spin-reorientation transition from out-of-plane to in-plane magnetization at ≈ 3.8 ML, two coexisting metastable spin configurations are found. [S0163-1829(99)10633-7]

I. INTRODUCTION

The reversal of magnetization in external magnetic fields in ultrathin magnetic films has attracted considerable interest recently.¹⁻³ This is mainly due to the potential novel applications in magnetic-storage and sensor technology, but also due to an interest in the complex process itself. The magnetization-reversal process is basically governed by domain nucleation in the vicinity of defects, steps, etc., with subsequent domain-wall motion, which is again strongly affected by film morphology and defects. Of particular interest is the magnetization-reversal process at or close to a spin-reorientation transition: In many systems, a transition from an out-of-plane to an in-plane easy axis of magnetization occurs at a specific film thickness (typically a few monolayers) and/or a specific temperature. At the transition, the magnetic anisotropies are rather small, which makes microdomain states (e.g., stripe domains) energetically favorable.⁴⁻⁷ However, states with uniform magnetization (out-of-plane, in-plane, or canted) can be stabilized in external magnetic fields and might be metastable in zero field giving rise to magnetic hysteresis.⁶⁻⁸

Magnetization reversal in ultrathin films is strongly affected by morphology on the nanometer scale,⁹ which makes it imperative to closely control growth and morphology of these films. Since a protective layer on top of an ultrathin magnetic film can have a strong influence on structure, morphology, and magnetism of the film, it is desirable to perform *in situ* measurements in ultrahigh vacuum (UHV). Considerable insight into the magnetization-reversal process can be obtained from magnetization curves (magnetic hysteresis loops), even though a knowledge of average magnetizations is often not sufficient to unambiguously interpret the reversal process. In this respect, a uniform canted magnetization cannot be distinguished from a domain state with the same average magnetization. For an improved understanding, it is therefore necessary to laterally resolve the film magnetization. Most of the available UHV-compatible domain-imaging techniques (based on scanning electron microscopy or magnetic force microscopy) are restricted to measurements at zero (or small) external magnetic field. On the other hand, Kerr microscopy, which is based on the magneto-optical

Kerr effect (MOKE), is well suited for measurements in external magnetic fields. At present, however, there are only a few UHV Kerr microscopes in operation.^{10,11}

In this article, we report on a combined study of low-temperature (LT) grown ultrathin films of Fe/Cu(100) by *in situ* Kerr microscopy, MOKE, and scanning tunneling microscopy (STM). The conclusions reached for this particular system concerning magnetization reversal in films with perpendicular magnetic anisotropy and spin reorientation are expected to be representative for several other systems. It is shown that the onset of long-range ferromagnetic order in Fe/Cu(100) is related to the coalescence of bilayer islands at ≈ 0.9 ML (a similar effect was previously found for Fe/W(110)).¹² For these very thin films, the shape of the magnetic hysteresis loop deviates from the squarelike shape observed for slightly thicker films, which is assigned to inhomogeneous film morphology and anisotropy. Domain nucleation and domain-wall motion during magnetization reversal in out-of-plane magnetized thin films could be imaged for films as thin as 1.9 ML. The observed strong influence of film thickness on coercive field and magnetic-domain shape is explained by thickness dependent magnetic anisotropy. Of particular interest is the coexistence of out-of-plane magnetized domains and domains with a reduced (or even vanishing) out-of-plane magnetization component at the spin-reorientation thickness of ≈ 3.8 ML. The latter may either have a uniform canted magnetization or an inner microdomain structure that is not resolved by the Kerr microscope.

II. EXPERIMENTAL DETAILS

The Fe/Cu(100) samples were prepared in a UHV system (base pressure: $< 3 \times 10^{-11}$ mbars) by electron-beam evaporation of Fe onto Cu(100) at 100 K. The deposition rate (≈ 1 Å/min) was measured by a quartz microbalance with an absolute error of $\pm 20\%$, and a relative reproducibility of $\pm 5\%$. Before deposition, Cu(100) was cleaned by more than 50 sputter-anneal cycles until a very sharp low-energy electron diffraction (LEED) pattern was obtained as well as wide and contamination-free Cu terraces were seen in the STM images.

The as-prepared samples were either transferred to a

custom-built UHV-STM operating at room temperature (RT) or into an interconnected UHV chamber specifically designed for *in situ* MOKE and Kerr-microscopy measurements. For Kerr microscopy, the sample and a UHV electromagnet were moved close to a $2\frac{3}{4}$ " view port, realizing the optimal working distance ($\cong 10$ cm) of the employed optical microscope (Questar QM100). The sample was illuminated by a Hg-discharge lamp, and a sheet polarizer and analyzer were placed in the incident and reflected beams, respectively. Images were recorded with a charge-coupled device (CCD) camera connected to an image-processing system that allows background subtraction and frame integration in order to eliminate topographical structures and enhance the signal-to-noise ratio, respectively. Only static domain images were recorded. To record domain images, the magnetization-reversal process was interrupted at certain points by slightly reducing the applied magnetic field. The lateral resolution of the Kerr microscope is about $3\ \mu\text{m}$. The MOKE and Kerr-microscopy measurements were performed in polar geometry, with the sample at 130 K, magnetized along the surface normal, and illuminated at a small angle ($\cong 10^\circ$) with respect to the surface normal. A detailed description of the Kerr microscope and the MOKE setup will be published elsewhere.¹³

III. RESULTS AND DISCUSSION

The system Fe/Cu(100) is known to exhibit strong relations between atomic structure and magnetic properties (see, e.g., Ref. 14 and references therein). For the first few monolayers (ML), which is the thickness range that is studied in the present work, Fe grows pseudomorphically on Cu(100) with a tetragonally distorted fcc structure (fct).¹⁵ In this thickness range the easy axis of magnetization is perpendicular to the surface (out-of-plane magnetization). We have grown the films at LT in order to obtain abrupt interfaces. RT-grown Fe/Cu(100) films exhibit strong Fe-Cu interdiffusion at the interface, which is expected to be suppressed at LT.¹⁶ For the as-grown films, a spin-reorientation from out-of-plane to in-plane magnetization is observed at 3.8 ML, which shifts to higher thickness (up to 6 ML) for annealed films.¹⁷

A. Onset of ferromagnetic order

Figure 1(a) shows an STM image of LT-grown 0.6-ML Fe/Cu(100), which is characterized by isolated bilayer islands with diameters ranging from $<10\ \text{\AA}$ to $>50\ \text{\AA}$; no MOKE signal could be detected from this film. At 0.9 ML, the bilayer islands coalesce [see Fig. 1(b)], and a polar-MOKE signal is recorded, indicating long-range magnetic order [hysteresis loops A and B in Fig. 1(c)]. Hysteresis loop A was taken before the sample was warmed up to RT for the STM measurements, loop B was recorded afterwards. Both loops were recorded at a temperature of 130 K. The RT-annealed film shows a higher MOKE signal and a larger coercive field. This is explained by a supposedly higher T_c resulting from a stronger coalescence of islands in the RT-annealed film, and hence a lower reduced temperature T/T_c leading to higher magnetization and magnetic anisotropy that will cause the observed changes in the hysteresis loop. Inter-

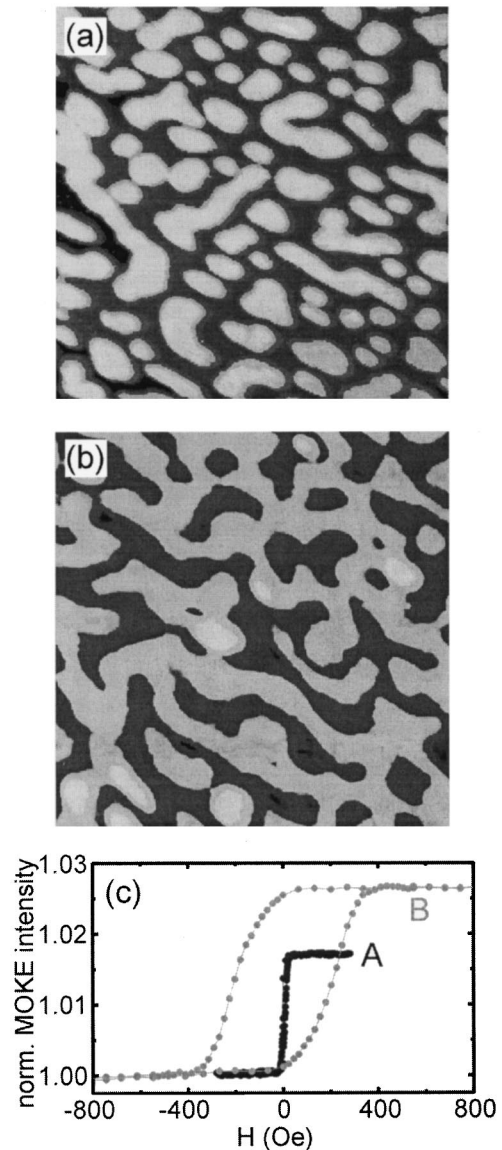


FIG. 1. (a) and (b): $400\times 400\ \text{\AA}$ STM images of (a) 0.6-ML and (b) 0.9-ML LT-grown Fe/Cu(100) exhibiting bilayer islands before and after coalescence. In (b), the nucleation of some 3-ML-high patches is observed. (c) Polar-MOKE hysteresis loops taken at 130 K of 0.9-ML Fe/Cu(100) annealed at (A) 130 K and (B) 300 K. The MOKE intensity is normalized to the respective lower signal; H is the external magnetic field.

estingly, loop B deviates considerably from a squarelike shape observed for thicker films (see below), which could well be caused by a locally varying degree of coalescence, i.e., a distribution of local coercive fields. Unfortunately, the magnetic contrast was too small to allow the recording of domain images. However, it is clear that the networklike film morphology, with structures on a nanometer scale, strongly affects the magnetization process.

It should be noted here that there is a controversy in the literature concerning the onset of long-range ferromagnetic order in LT-grown Fe/Cu(100) films, ranging from about 1 ML to more than 2 ML.^{6,18,19} The present data clearly shows that at 130 K ferromagnetism occurs even below 1 ML. One reason why in some studies a delayed onset of ferromagnetism was found could be that in these cases the films were

magnetized by short magnetic-field pulses, which were either not strong enough to overcome the rather large coercive field (as compared to thicker films, see below) or too short to allow for domain-wall motion.

B. Magnetization reversal in out-of-plane magnetized films

In the following, the magnetization-reversal process in 1.9-ML and 3.2-ML-thick Fe/Cu(100) films is discussed. In Figs. 2(a) and 2(b), the hysteresis loop for a 1.9-ML-thick film is shown as well as a set of domain images taken during magnetization reversal in magnetic fields close to the coercive field $H_C = 80$ Oe. The hysteresis loop has square shape, and the magnetization-reversal process is characterized by nucleation of only few domains with reversed magnetization (dark areas in the images) followed by continuous domain growth. Note that the domain walls are rather straight. At 3.2 ML Fe/Cu(100), the hysteresis loop retains its square shape but the coercive field is reduced to $H_C = 32$ Oe [see Fig. 2(a)]. Furthermore, the magnetic domains forming during magnetization reversal [see Fig. 2(c)] have a completely different shape than those for 1.9 ML: There are numerous nucleation centers, and the domains have an irregular shape, since they are pinned at several points of the film. Nucleation centers and pinning sites correspond to crystal defects and polishing scratches on the Cu(100) surface as is seen by comparing the magnetic-domain images with the background-topography image (not shown here).

Domain nucleation and wall motion in these Fe/Cu(100) films is governed by thermal activation, and the wall velocity depends exponentially on the external magnetic field.^{10,20} A squarelike hysteresis shape usually indicates that the coercive field is determined by the magnetic field necessary for a domain nucleation that triggers an almost instantaneous magnetization reversal. In the present case, however, the coercive field is given by the field at which domain-wall motion occurs on the time scale of the hysteresis-loop data recording (in the order of 1 s). Therefore the squareness of the hysteresis loops is a measure for the homogeneity of the films. At this point it should be mentioned that the investigated films are fairly smooth, with the roughness increasing towards larger thicknesses [see STM images in Figs. 2(d) and (e)]. The lateral size of islands and holes is of the order of 1–3 nm. From annealing studies where the nanometer-scale morphology of 1.9-ML and 3.2-ML-thick Fe/Cu(100) films was altered we do not get any indication that magnetization reversal is affected by roughness on this small length scale, probably because the domain-wall widths exceed this scale. A detailed discussion of the influence of film morphology on the magnetization-reversal process will be published elsewhere.¹³ Barriers for domain-wall propagation are more likely to be represented by Cu(100)-surface steps and defects on the Cu surface.¹⁰ For the 0.9-ML Fe/Cu(100) film, on the other hand, it is possible that anisotropies are large enough to lead to sufficiently small domain-wall widths. In this case, the networklike film morphology [see Fig. 1(b)] would have a strong impact on the magnetization-reversal process, which remains to be studied.

We will now address the observed thickness dependence of coercive field and domain shapes during magnetization reversal: A reduction of H_C is commonly observed in ultra-thin magnetic films by approaching the spin-reorientation

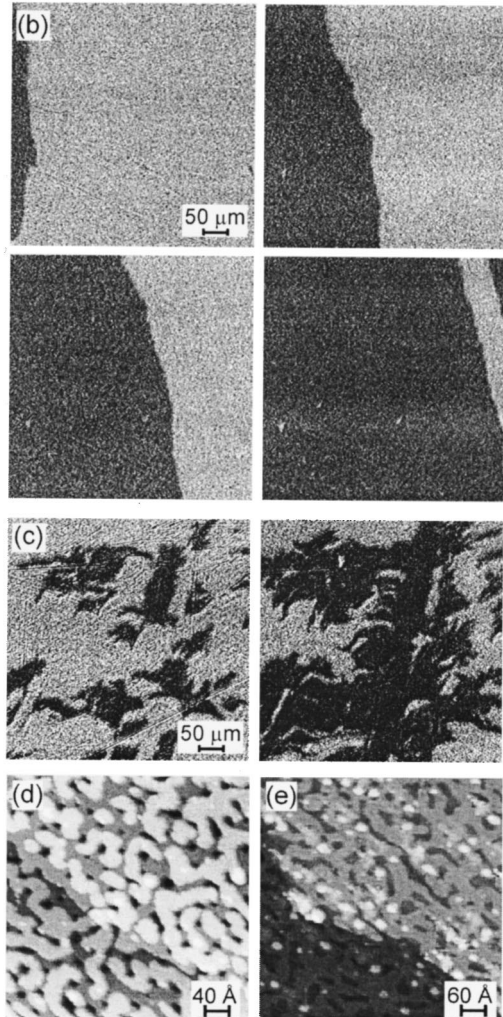
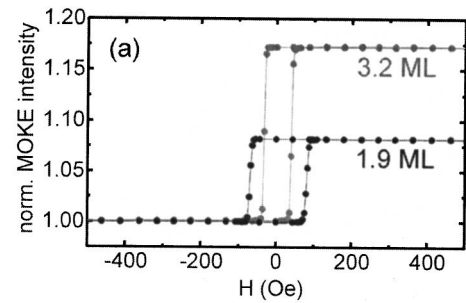


FIG. 2. (a) Polar-MOKE hysteresis loops of LT-grown 1.9-ML and 3.2-ML Fe/Cu(100) taken at 130 K. (b) and (c): Corresponding series of magnetic-domain images taken during magnetization reversal around the coercive fields at (b) 1.9-ML and (c) 3.2-ML Fe/Cu(100). The dark areas indicate domains with reversed out-of-plane magnetization. (d) and (e): STM images of (d) 1.9-ML and (e) 3.2-ML Fe/Cu(100). The islands protrude typically 1 ML out of the surface while some holes are at least 2-ML deep and reach down to the Fe-Cu interface.

thickness.¹ It is assigned to a decrease of the magnetic anisotropy (which is supposed to almost vanish at spin reorientation) resulting in lower energy thresholds for domain nucleation and domain-wall motion. The observation of such strong changes in domain shape, however, is interesting. It is explained by a reduced domain-wall energy caused by a diminished magnetic anisotropy. To first approximation, the

magnetic anisotropy E_a can be written as: $E_a = K_2 \cos^2 \theta = (K_{b,2} + K_{s,2}/d) \cos^2 \theta$, where θ is the angle between magnetization direction and surface normal, d is the film thickness, and $K_{b,2}, K_{s,2}$ are second-order anisotropy constants for bulk and surface, respectively. $K_{b,2}$ is positive and includes the shape-anisotropy term $1/2 \mu_0 M^2$ with M being the magnitude of the saturation magnetization. For Fe/Cu(100), the surface-anisotropy term is negative, which explains the perpendicular anisotropy of thin films. Since the anisotropy changes sign at the spin-reorientation thickness $d_0 \cong 3.8$ ML (Ref. 21) (see discussion below), it follows that $K_{s,2} \cong -d_0 K_{b,2}$. The domain-wall energy per unit length, γ , depends on K_2 , d , and the exchange stiffness A in the form $\gamma \propto d \cdot (A|K_2|)^{1/2} = (AK_{b,2}|dd_0 - d^2|)^{1/2}$. There is a maximum in $\gamma(d)$ at $d = d_0/2 \cong 1.9$ ML, and a minimum at $d_0 \cong 3.8$ ML. For the domain growth at 3.2-ML Fe/Cu(100), the energy barrier for introducing longer domain walls is obviously smaller than the barrier height for domain walls to overcome pinning centers, which explains the observed rugged domain shapes. For 1.9-ML Fe/Cu(100), on the other hand, the domain walls tend to be as short as possible, in agreement with the rather straight domain boundaries. It should be noted that the observed, differently shaped domains are not representing thermodynamical ground states. They are a consequence of the dynamical, thermally activated process of domain-wall motion. It should also be mentioned that in the discussion of domain shapes the influence of long-range magnetic dipole-dipole interaction (magnetostatic energy) can be neglected: The domains are typically much wider than $10 \mu\text{m}$ which is beyond the scale where—at a film thickness of less than 1 nm—significant variations in the magnetostatic energy occur.⁶

C. Spin reorientation

In the last section, the magnetization-reversal process at the spin-reorientation transition is discussed. The hysteresis loop of a 3.8-ML Fe/Cu(100) film [see Fig. 3(a)] shows that there is still almost 100% remanence, but the hysteresis loop no longer has square shape. Interestingly, rather similar hysteresis loops were observed at the spin-reorientation transition of Fe/Cu₃Au(100).²² Without domain imaging, however, there could only be a speculation on the nature of the magnetization-reversal process. With Kerr-microscopy [see Figs. 3(b) and (c)], it is now seen that the magnetization reversal starts with nucleation of magnetic domains that are even more irregularly shaped than that in case of 3.2-ML Fe/Cu(100), in consistency with the preceding discussion. However, the magnetic contrast is lower than observed for 3.2-ML Fe/Cu(100). Upon reaching an apparent single-domain state,²³ the magnetic contrast increases further with higher external magnetic fields up to the saturation field $H_0 \cong 200$ Oe. To demonstrate the magnetic contrast effects more clearly, the external magnetic field was reduced before a single-domain state had been established (inner hysteresis loop). In this case, the domain contrast diminished continuously and reversibly with decreasing (and increasing reversed) external magnetic field [compare Figs. 3(c) and (d)], with the domain walls at an apparently fixed position. The corresponding inner hysteresis loop is not plotted in Fig. 3(a)

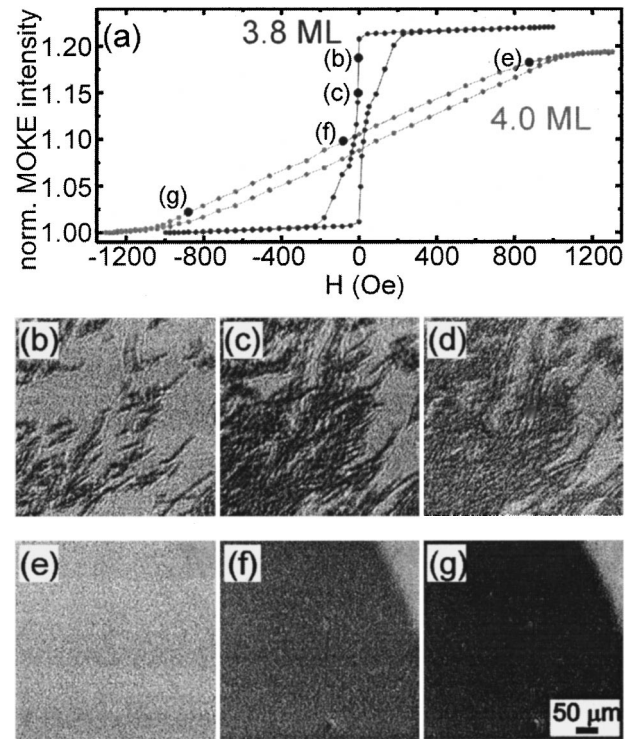


FIG. 3. (a) Polar-MOKE hysteresis loops for (A) 3.8-ML and (B) 4-ML Fe/Cu(100). The approximate points at which domain images were recorded are indicated. (b) and (c): Growth of magnetic domains (dark areas) for 3.8-ML Fe/Cu(100). (d) After a domain state similar to that in (c) had established, the external magnetic field was reduced to $H \cong 0$ resulting in less magnetic contrast in the dark areas. (e)–(g): Domain images during magnetization reversal at 4-ML Fe/Cu(100). In the upper-right corner the nonmagnetic sample holder is seen.

since the average film magnetization cannot be determined accurately from the domain images.

The spin-reorientation phase transition occurs within a rather narrow thickness range (< 0.5 ML): Already at a 4-ML-thick Fe/Cu(100) film, an almost hard-axis hysteresis loop is measured [though there is still some hysteresis effect, see Fig. 3(a)]. Accordingly, the magnetic contrast in Kerr-microscopy images changes continuously for magnetic fields below the saturation field, and no domain nucleation processes are observed [see Figs. 3(e)–(g)].

Lower magnetic contrast of domains in Kerr-microscopy images taken at 3.8-ML Fe/Cu(100) [dark areas in Figs. 3(b)–(d)] is directly attributed to a reduced out-of-plane magnetization component within the domains. The domains are either in a uniform canted magnetization state (including in-plane magnetization at or near zero external magnetic field) or in a microdomain state with a nonresolved inner domain structure. In any case, the domains exhibit a different spin structure than the surrounding areas with uniform out-of-plane magnetization stabilized in an external magnetic field prior to magnetization reversal [bright areas in Figs. 3(b)–(d)]. Both models are discussed in more detail in the following.

It is known that at the spin-reorientation transition microdomain states become energetically favorable due to a diminished magnetic anisotropy and a gain in dipole energy.⁶

Due to this fact, hysteresis loops measured at Fe/Cu₃Au(100) with shapes like that in Fig. 3(a) for 3.8-ML Fe/Cu(100) were previously attributed to a transition from a metastable out-of-plane magnetization state that persists in zero external magnetic field (remanence) to a microdomain state at a sufficiently large reversed external magnetic field.²² The net magnetization of a thermodynamically stable microdomain state would be zero at zero external magnetic field and increase with field. The energy of the domain walls that have to be created at the transition represents an activation barrier and explains why the out-of-plane state is metastable. So far, this model is consistent with the present Kerr-microscopy data since microdomain states (e.g., stripe domains with stripe widths $< 1 \mu\text{m}$) are not resolved, and the changing magnetic contrast in the Kerr-microscopy images would just reflect the net magnetization of the microdomain state. The Kerr-microscopy images in Figs. 3(b) and (c) imply that after nucleation the possible microdomain phase grows by domain-wall displacement rather than entirely by nucleation. Therefore it could be expected that the domains have more a fractal-like shape^{2,24} rather than a stripelike configuration.⁶

There is one point which is not in accordance with previous theoretical and experimental studies of microdomain states, though: Small external magnetic fields (< 50 Oe) should already destabilize the microdomain state and cause a transition to an out-of-plane magnetized single-domain phase.^{6,8} In the present case, however, the transition field amounts to about 200 Oe [see hysteresis loop for 3.8-ML Fe/Cu(100) in Fig. 3(a)]. This fact leads to the assumption that at 3.8 ML, the effective second-order magnetic anisotropy constant K_2 has already changed sign ($K_2 > 0$), favoring in-plane magnetization.²⁵ Provided that the out-of-plane magnetized state is still metastable, the nucleated domains observed in the Kerr-microscopy images [Figs. 3(b)–(d)] would have uniform in-plane magnetization, in contrast to the preceding discussion. The inclined straight sections in the hysteresis loop [Fig. 3(a)] and the changing magnetic contrast in the Kerr-microscopy images [Figs. 3(c) and (d)] would result from a coherent rotation of the magnetization in the external magnetic field (canted spin orientation). Interest-

ingly, one recent study by Speckmann, Oepen, and Ibach suggests the coexistence of the out-of-plane and in-plane magnetization phase in remanence at the spin-reorientation transition of Co/Au(111).⁷ Experimentally, they show that a metastable out-of-plane single-domain state exist. It remains unclear, however, whether also the in-plane domain state can be stabilized. The coexistence of the two phases is explained by taking higher-order contributions to the magnetic anisotropy into account. Indeed, the importance of higher-order anisotropies at the spin-reorientation transition was pointed out in recent works.^{7,26}

On the basis of the present data alone, we cannot give a conclusive answer to the question of the spin configuration within the domains with a reduced out-of-plane magnetization component observed at 3.8-ML Fe/Cu(100)—whether it is uniform or exhibits a microdomain structure. A better theoretical understanding of domain formation in external magnetic fields as well as domain-imaging studies with improved lateral resolution are required. For this purpose, we are currently developing a UHV scanning near field optical microscope (SNOM) for magnetic-domain imaging with submicron resolution.²⁷

IV. SUMMARY

In summary, we have investigated the magnetization reversal process in external magnetic fields at low-temperature grown Fe/Cu(100) films for film thicknesses up to 4 ML. With a combined *in situ* MOKE, Kerr microscopy, and STM study we were able (i) to attribute the onset of long-range ferromagnetic order to the coalescence of bilayer islands at about 0.9 ML, (ii) to assign the irregular domain shapes above 3 ML to a reduced domain-wall energy, and (iii) to identify two coexisting spin configurations at the spin-reorientation transition that occurs in a narrow thickness range around 3.8 ML.

ACKNOWLEDGMENT

This work was supported by the Deutsche Forschungsgemeinschaft, Project No. Sfb-290/TPA6.

¹P. Bruno, G. Bayreuther, P. Beauvillain, C. Chappert, G. Lugert, D. Renard, J. P. Renard, and J. Seiden, *J. Appl. Phys.* **68**, 5759 (1990).

²A. Lyberatos, J. Earl, and R. W. Chantrell, *Phys. Rev. B* **53**, 5493 (1996).

³A. Moschel, R. A. Hyman, A. Zangwill, and M. D. Stiles, *Phys. Rev. Lett.* **77**, 3653 (1996).

⁴D. P. Pappas, K.-P. Kämper, and H. Hopster, *Phys. Rev. Lett.* **64**, 3179 (1990).

⁵R. Allenspach and A. Bischof, *Phys. Rev. Lett.* **69**, 3385 (1992).

⁶Y. Yafet and E. M. Gyorgy, *Phys. Rev. B* **38**, 9145 (1988); A. B. Kashuba and V. L. Pokrovsky, *ibid.* **48**, 10 335 (1993).

⁷M. Speckmann, H. P. Oepen, and H. Ibach, *Phys. Rev. Lett.* **75**, 2035 (1995); H. P. Oepen, M. Speckmann, Y. Millev, and J. Kirschner, *Phys. Rev. B* **55**, 2752 (1997).

⁸A. Berger and H. Hopster, *Phys. Rev. Lett.* **76**, 519 (1996); A.

Berger and R. P. Erickson, *J. Magn. Magn. Mater.* **165**, 70 (1997).

⁹D. Sander, R. Skomski, C. Schmidhals, A. Enders, and J. Kirschner, *Phys. Rev. Lett.* **77**, 2566 (1996).

¹⁰A. Kirilyuk, J. Giergiel, J. Shen, and J. Kirschner, *J. Magn. Magn. Mater.* **159**, L27 (1996).

¹¹A. Vaterlaus, U. Maier, U. Ramsperger, A. Hensch, and D. Pescia, *Rev. Sci. Instrum.* **68**, 2800 (1997).

¹²H. J. Elmers, J. Hauschild, H. Höchle, U. Gradmann, H. Bethge, D. Heuer, and U. Köhler, *Phys. Rev. Lett.* **73**, 898 (1994).

¹³E. Mentz, A. Bauer, and G. Kaindl (unpublished).

¹⁴S. Müller, P. Bayer, C. Reischl, K. Heinz, B. Feldmann, H. Zillgen, and M. Wuttig, *Phys. Rev. Lett.* **74**, 765 (1995).

¹⁵H. Magnan, D. Chandesris, B. Vilette, O. Heckmann, and J. Lecante, *Phys. Rev. Lett.* **67**, 859 (1991).

¹⁶D. A. Steigerwald, I. Jacob, and W. F. Egelhoff, *Surf. Sci.* **202**, 472 (1988).

- ¹⁷E. Mentz, D. Weiss, J. E. Ortega, A. Bauer, and G. Kaindl, *J. Appl. Phys.* **82**, 482 (1997).
- ¹⁸D. Li, M. Freitag, J. Pearson, Z. Q. Qiu, and S. D. Bader, *Phys. Rev. Lett.* **72**, 3112 (1994).
- ¹⁹D. P. Pappas, C. R. Brundle, and H. Hopster, *Phys. Rev. B* **45**, 8169 (1992).
- ²⁰E. Fatuzzo, *Phys. Rev.* **127**, 1999 (1962).
- ²¹H. Zillgen, B. Feldmann, and M. Wuttig, *Surf. Sci.* **321**, 32 (1994).
- ²²F. Baudelet, M. T. Lin, W. Kuch, K. Meinel, B. Choi, C. M. Schneider, and J. Kirschner, *Phys. Rev. B* **51**, 12 563 (1995).
- ²³Polar MOKE measures only the out-of-plane magnetization component so that domains with different in-plane spin orientation cannot be distinguished by polar Kerr microscopy.
- ²⁴J. Valentin, Th. Kleinefeld, and D. Weller, *J. Phys. D* **29**, 1111 (1996).
- ²⁵This possibility was also discussed in Ref. 22 and dismissed since no MOKE signal was detected in longitudinal geometry, which would be expected if the easy axis is in plane. For a better understanding, longitudinal MOKE measurements would have to be done here as well.
- ²⁶K. Baberschke and M. Farle, *J. Appl. Phys.* **81**, 5038 (1997).
- ²⁷B. L. Petersen, A. Bauer, G. Meyer, T. Crecelius, and G. Kaindl, *Appl. Phys. Lett.* **73**, 538 (1998).